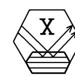

DIFFUSE X-RAY SCATTERING FROM DEFECTS IN Si SINGLE CRYSTALS MEASURED AT VARIOUS TEMPERATURES

V. Valeš[1] and V. Holý[2,1]

[1]Insitute of Condensed Matter Physics, Faculty of Science, Masaryk University, Kotlářská 2, CZ – 61137 Brno, Czech Republic,

[2]Department of Condensed Matter Physics, Faculty of Mathematics and Physics, Charles University, Ke Karlovu 5, 121 16 Praha, Czech Republic,

106575@mail.muni.cz

Keywords:
diffuse X-ray scattering, thermal diffuse scattering, defects, silicon

Abstract

Diffuse X-ray scattering from defects in Czochralski-grown Si wafers (small stacking faults, precipitates of SiO_2, clusters of vacancies or interstitials) is measured at two different temperatures. From the comparison of the reciprocal-space distributions of the intensity scattered at different temperatures we have determined the thermal-diffuse part and the part of the intensity scattered from the structural defects. Since the intensity of thermal diffuse scattering is not affected by the presence of the defects, it can be used as an internal intensity normal. This made it possible to determine reliably the density of structure defects in the wafers.

1. Introduction

Defects in Czochralski-grown Si crystal play a crucial role in semiconductor technology. They may be detrimental and unfavorably affect the electric properties of semiconductor structures, or they can have a beneficial role as gettering centers that decrease the density of heavy metal atoms. Therefore, a detailed characterization of the defect nature, their sizes and densities, is of a substantial importance.

Several methods are used for the defect characterization, wet chemical etching, transmission electron microscopy (TEM), and X-ray diffraction, among others. X-ray diffraction method is usually based on the measurement of the distribution of X-ray intensity diffusely scattered from the defects in reciprocal space close to a suitably chosen reciprocal lattice point. In contrast to TEM, the method is indirect, i.e. it cannot yield a direct depiction of the defects, and the measured intensity distribution must be compared to numerical simulations. On the other hand, the parameters of the defects obtained by this way have much better statistical relevance than those from TEM, since the primary X-ray beam irradiates a large number of defects and the measured signal is usually averaged over a statistical ensemble of all defect configurations.

Theory of diffuse X-ray scattering is based on kinematical scattering theory and on a statistical averaging and it is thoroughly explained in a series of papers (see the seminal monograph [1], for instance). From the theory it follows that the diffusely scattered intensity is proportional to the number of irradiated defects, i.e., on the defect density. Therefore, a reliable determination of the defect density is rather complicated, since an *absolute* measurement of the scattered intensity is necessary. This is a complicated task, since the absolute value of the scattered intensity is affected by a number of experimental parameters (angular divergence of the primary beam, size of the beam and its wavelength spread, as well as the angular resolution of the analyzing crystal, etc.).

Fortunately, the intensity of diffuse scattering from defects can be compared with the intensity of thermal diffuse scattering (TDS), which acts as an *internal intensity normal* that is not affected by the presence of defects [2]. Usually, using conventional laboratory equipment for high-resolution X-ray diffraction, it is not easy to measure TDS at room temperature, since its intensity disappears in the experimental background. The idea of this work is to enhance the TDS intensity by increasing the sample temperature, which helps us to identify unambiguously the TDS contribution to the diffusely scattered intensity. It could also make it possible to determine the defect density in samples, where the TDS intensity at the room temperature disappears in the experimental background. In order to test this idea, we measure the diffuse scattering at an elevated temperature from a sample, in which the TDS intensity can be measured at room temperature as well.

The paper is organized as follows. In the next section we summarize the basic formulas and ideas of diffuse scattering from defects and of the TDS, the theory has been taken from [1, 3, 4]. Section 3 contains experimental results their discussion.

2. Theory

In the following we use a simplified defect model, in which a defect in crystal consists of two parts – the defect core, where the structure is much different than in the surrounding crystal, and the deformed area of the crystal matrix around the defect core. It is evident that the polarizability coefficients $_g$ of the defect core are different from those of the crystal without defects. As for the deformed area around the core, we assume that the polarizability coefficients $_g$ do not differ from those of a non-deformed crystal. The expression for the reciprocal distribution of the diffusely scattered intensity is (see [1,3])

$$J(\boldsymbol{q}) \quad I_i \frac{K^6 t}{16\ ^2}\exp(\ 2M) \quad n \ |\ ^{FT}(\boldsymbol{q})|^2 , \qquad (1)$$

where t is the sample thickness, M is the thermal Debye Waller factor, the sum over goes over the types of de-

fects, n is the volume density of defects of type and the function,

$$^{FT}(\boldsymbol{q}) \quad d^3\boldsymbol{r} \quad (\boldsymbol{r})\exp(\ i\boldsymbol{q} \ \boldsymbol{r})$$

is the Fourier transformation of the structure factor ($\boldsymbol{r}$) of a defect of type , described later. $\boldsymbol{q}$ is the reduced scattering vector ($\boldsymbol{q} = \boldsymbol{Q} \quad \boldsymbol{h}$), where $\boldsymbol{h}$ is the diffraction vector and $\boldsymbol{Q}$ is the scattering vector (the difference of the wave vectors of the scattered and primary x-ray beams).

The structure factor of a defect is a sum of two contributions describing the scattering from the elastically deformed defect neighborhood (the Huang scattering) and from the defect volume (the core scattering). The structure factor of the Huang scattering is [1, 3]

$$_{Huang}(\boldsymbol{r}) \quad _h[1 \quad \exp(\ \boldsymbol{h} \quad (\boldsymbol{r}))] \tag{2}$$

where v ($\boldsymbol{r}$) is the displacement field around a defect of type lying in the origin $\boldsymbol{r} = 0$. If the displacements of the atoms around the defect core are much smaller then 2 /|$\boldsymbol{h}$|, we can approximate Eq. (2) by

$$_{Huang}(\boldsymbol{r}) \quad i \ _h\boldsymbol{h} \quad (\boldsymbol{r}) \tag{3}$$

The structure factor of the core scattering is [2]

$$_{Core}(\boldsymbol{r}) \quad _h \quad (\boldsymbol{r})\exp(\ i\boldsymbol{h} \quad (\boldsymbol{r})), \tag{4}$$

where $_h$ is the difference between polarizability coefficients of the defect core and of the surrounding crystal, and is the shape function of a defect of type (unity in the defect volume and zero outside it).

Another type of diffuse scattering, which affects the $\boldsymbol{q}$-dependence of the diffuse scattering, is the thermal diffuse scattering (TDS), in which the X-ray photons are scattered by phonons. TDS is not affected by defects in the crystal structure and the first approximation of its intensity (up to the first power of the absolute temperature T) reads [3, 4]

$$J_{TDS}(\boldsymbol{q}) \quad I_i \frac{K^6 t}{16 \ ^2}| \ _h|^2 \exp(\ 2M)\frac{k_b T}{q^2} \ _p \ \frac{(\boldsymbol{h} \ \boldsymbol{e}_{qp})^2}{_{qp}} \tag{5}$$

where T is the absolute temperature, k_B is the Boltzmann constant, the sum runs over the branches of the phonon band structure, $\boldsymbol{e}_{qp}$ is the unit polarization vector of a p-th phonon with the wave vector $\boldsymbol{q}$, and $_{qp}$ are the eigenvalues of the matrix

$$A_{jm}(\boldsymbol{q}^0) \quad C_{jkmn}q_k^0 q_n^0, j,k,m,n \quad x,y,z\,. \tag{6}$$

Here C_{jkmn} are the elasticity coefficients of the crystal and $\boldsymbol{q}^0$ is the unit vector parallel to $\boldsymbol{q}$. The eigenvalues $_{qp}$ are connected with the phase velocities of the acoustic phonons c_{qp}

$$_{qp} \quad c_{qp}^2 q^2 \ ,$$

where is the crystal mass density. The polarization vectors $\boldsymbol{e}_{qp}$ are the corresponding eigenvectors of the matrix .

From Eqs. (1) and (6) it follows that the ratio of the static diffuse scattering (i.e., the scattering from defects) with the TDS is

$$\frac{J(\boldsymbol{q})}{J_{TDS}(\boldsymbol{q})} \quad n\frac{| \ ^{FT}(\boldsymbol{q})|^2}{\frac{k_b T}{q^2} \ _h|^2 \ _p \ \frac{(\boldsymbol{h} \ \boldsymbol{e}_{qp})^2}{_{qp}}} \tag{7}$$

if we assume that only one defect type is present in the crystal. From this ratio we can determine the density n of these defects, since all the unknown parameters such as the primary intensity I_i, the resolution function of the diffractometer, etc. cancelled out.

As an illustration, we calculate the static diffuse scattering from a crystal containing randomly distributed spherical inclusions with radius R = 10 nm. Figure 1(a) shows the reciprocal space map of diffusely scattered intensity $J(\boldsymbol{q})$ calculated around the reciprocal lattice point 004, the axes q_x and q_z are along [100] and [001], respectively. In Fig. 1(b) we have plotted the cut of the calculated reciprocal space map along the q_z-axis. In this figure, we can distinguish two regions on the curve $J(q_z)$. For small q the Huang scattering dominates. Calculating its intensity, we perform the Fourier transformation of the structure factor $_{\text{Huang}}(\boldsymbol{r})$, and for the value of $^{FT}_{Huang}(\boldsymbol{q})$ for small $\boldsymbol{q}$, the values of for large |$\boldsymbol{r}$| are important. Therefore, for the calculation of the diffusely scattered intensity for small $\boldsymbol{q}$ we use Eq. (3) for the structure factor and the asymptotic displacement field $\boldsymbol{v}(\boldsymbol{r})$ for large $\boldsymbol{r}$. For any kind of defect, the asymptotic displacement field has the form

$$_j(\boldsymbol{r}) \quad P_{jk}\frac{x_k}{r^3}, j,k \quad x,y,z \tag{8}$$

where P_{jk} is the dipole force tensor of the defect (see [1,5], among others), the form of which depends on the defect nature. The Fourier transformation of the structure factor is

$$^{FT}_{Huang}(\boldsymbol{q}) \quad 4 \quad _h \frac{P_{jk}h_j q_k}{q^2} \tag{9}$$

and therefore the intensity of the Huang scattering is proportional to q . For large q, the scattering from the defect cores dominates. In this region, the calculated scattered intensity exhibits oscillations, which period depends on the defect size. Usually, the sizes of the defects are statistically distributed, so that the core scattering is represented by a smooth curve proportional to q .

In Fig. 1(b) we have also schematically plotted the intensity $J_{TDS}(\boldsymbol{q})$ of the thermal diffuse scattering. From Eq. (5) it follows that similarly to the Huang scattering. The absolute value of $J_{TDS}(\boldsymbol{q})$ depends on the defect density.

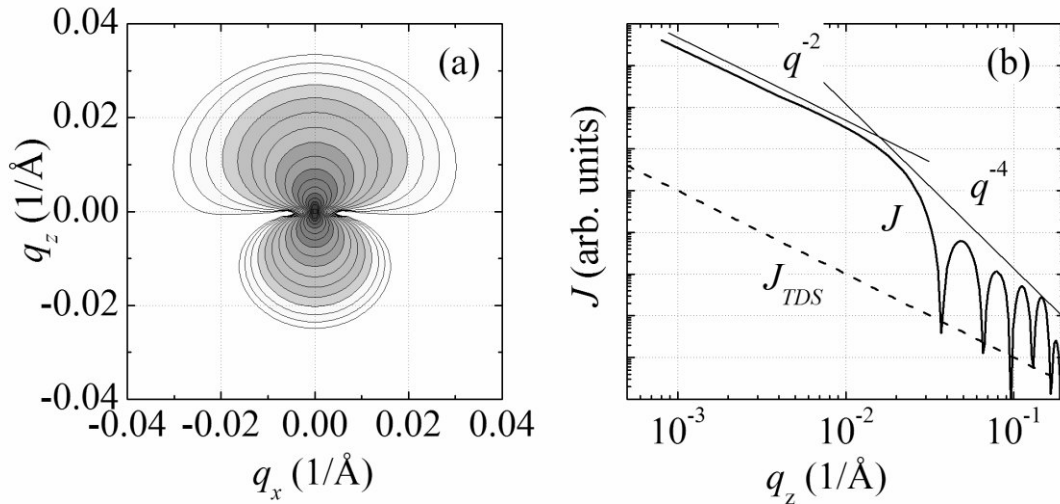

Figure 1. The reciprocal space map of diffusely scattered intensity calculated around the 004 reciprocal lattice point for randomly distributed spherical inclusions of radius 10 nm elastically deforming the neighboring lattice (a) and the cut of the map along the q_z-axis (b).

3. Experimental results

We have used the approach described above for the estimation of the defect density in a (111)Si wafer grown by the Czochralski method and subjected to the following four annealing steps: (i) 1000° C for 15 min, (ii) 600° C for 8 hours, (iii) 800° C for 4 hours, and finally (iv) 1000° C for 16 hours. The first annealing is used to achieve the homogeneity of the distribution of point defects in the sample volume, during the steps (ii) and (iii) nuclei of defects are created, and the defects grow during the annealing step (iv). The kinetics of the nucleation and growth of the defects during these annealing steps has been investigated theoretically and experimentally in [6].

For the measurement of diffuse x-ray scattering at room temperature we have used a high-resolution diffractometer, consisting of a standard X-ray tube (long fine focus, Cu target, 2 kW), a parabolic multilayer X-ray mirror followed by a 4 Ge220 Bartels monochromator. Under usual experimental conditions, the intensity of the primary beam was approx 5.10^5 cps, its size was about 0.5 3 mm^2, and divergence of about 12 arcsec. The scattered radiation passed through a channel-cut analyzer (2 Ge220) and its intensity was detected by a standard scintillation counter. For high-temperature measurements we have used a low-resolution diffractometer setup, in which the primary beam was collimated and partially monochromatized by a parabolic X-ray multilayer mirror, and the scattered beam was analyzed by a pair of plane X-ray multilayer mirrors in the disperse geometry. In this setup, the divergence of the primary beam was approx 1.5 arcmin and its intensity was approx. 2.10^6 cps. The sample was mounted on a horizontal heater in a small vacuum chamber, the sample temperature was measured by a thermocouple attached to the heater. In both experimental setups, the measured intensity was integrated along the q_y-axis, i.e., there was no resolution in reciprocal space in direction perpendicular to the $q_x q_z$ scattering plane.

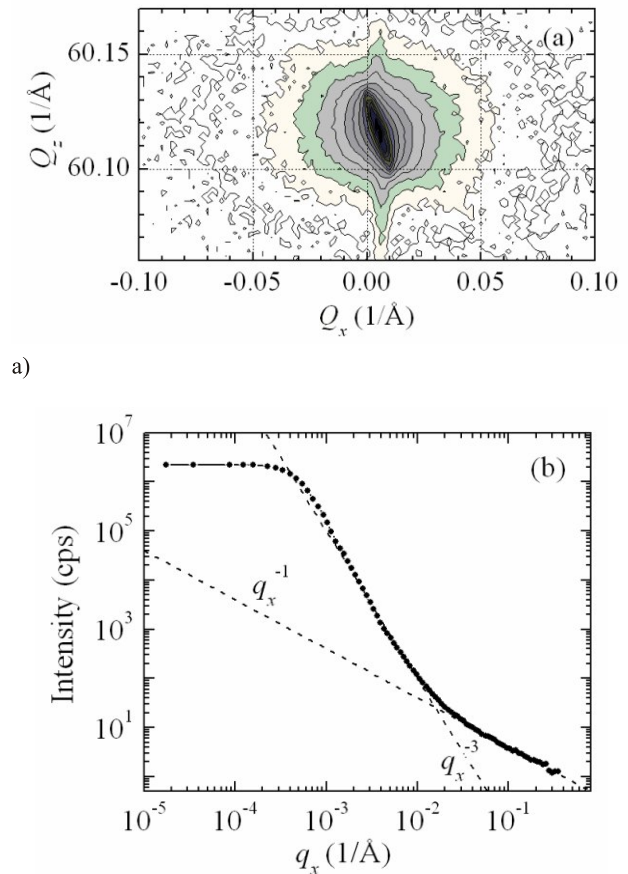

Figure 2. Reciprocal-space map of diffuse intensity measured in symmetric diffraction 333 (a) and the q_x-scan extracted from the map (b). Two regions with slopes –1 and –3 are visible.

We have measured reciprocal-space maps of scattered intensity around a symmetric reciprocal lattice point 333 at room temperature and line scans in reciprocal space parallel to the q_x-axis at 650° C. Figure 2(a) shows the reciprocal-space map measured at room temperature, in Fig. 2(b)

we have plotted the line scan extracted from this map parallel to the q_x-axis, crossing the intensity maximum. In the log-log representation of this scan we can distinguish three regions. For $q_x < 5.10^{4}$ Å^{1} the intensity is almost constant – this region corresponds to the experimental width of the crystal truncation rod, i.e., to the reciprocal-space resolution of the experimental setup. Between 5.10^{4} Å^{1} and 10^{2} Å^{1} the measured intensity drops as q_x^{3}, and above 10^{2} Å^{1} the intensity decreases as q_x^{1} until an experimental background is reached.

The q_x^{3}-region stems for the core scattering. In the previous section we have shown that the intensity of core scattering decreases as q , after the integration over q_y due to the lack of resolution in this direction we obtain J_{core} q_x^{3}. In the measured data, the Huang region cannot be resolved. Most likely, the defects do not deform the surrounding lattice so that the Huang scattering is very weak and the defects are quite large so that their mean size can be compared to the coherence width of the primary x-ray beam; in further simulations we assumed the mean defect diameter of $2R = 0.5$ m. In the q_x^{1}-region TDS is predominant; again, the q_y-integration decreases the slope of the TDS scattering from q to q .

Using the procedure described above, we compared the intensities of the core scattering and TDS scattering and from Eq. (7) we estimated the density of the defects to $n = (4 \pm 2).10^{7}$ cm^{3}. In the simulation of the intensity of core scattering we took the mean defect size mentioned above and we assumed that the defect volumes do not diffract, i.e., in Eq. (4) we put $_h$ $_h$.

Figure 3 compares the q_x-scans measured at room temperature and at 650° C. From the figure it follows that the core regions of the scans measured at two temperatures coincide; the TDS region is enhanced at the elevated temperature, indeed. The small discrepancy at q_x Å^{1} is probably a geometrical artifact; it may be caused by Be windows in our high-temperature chamber.

From the figure it also follows that the slope of the TDS regions measured at different temperatures are different; at room temperature the slope corresponds to the theory summarized in the previous section, and at the elevated temperature the slope is approx. 1.5. The reason for this difference is not clear. The different slopes of the measured TDS curves make it impossible to compare directly the TDS intensities and to check the validity of Eq. (5). From the ratio of the TDS intensities measured at $q_x = 0.03$ Å^{1} we have estimated the actual temperature of the sample to (500 ± 50)° C. Therefore, the TDS measurement can be used as a thermometer determining the actual sample temperature.

A further increase of the sample temperature during the measurement of diffuse scattering would enhance the TDS intensity but such an annealing step would modify the structure of the defects. The temperature 650° C used in the measurement is the maximum temperature, for which changes in the structure of the defects can be neglected.

4. Summary

We have measured the reciprocal-space distribution of diffuse X-ray scattering from small defects in a Czochralski-grown Si wafer after heat treatment. In the intensity scan along a straight line in reciprocal space we have distinguished the diffuse scattering from the defect cores from thermal diffuse scattering (TDS); the latter increases with increasing sample temperature. The intensity TDS served as an internal intensity normal to which the core scattering intensity can be normalized. This procedure made it possible to determine the defect density without normalizing the intensity of diffuse scattering to the primary intensity. We have successfully tested the idea of enhancing TDS by increasing the sample temperature. This procedure makes it possible to determine the density of defects also in samples, in which the TDS is not measurable at room temperature.

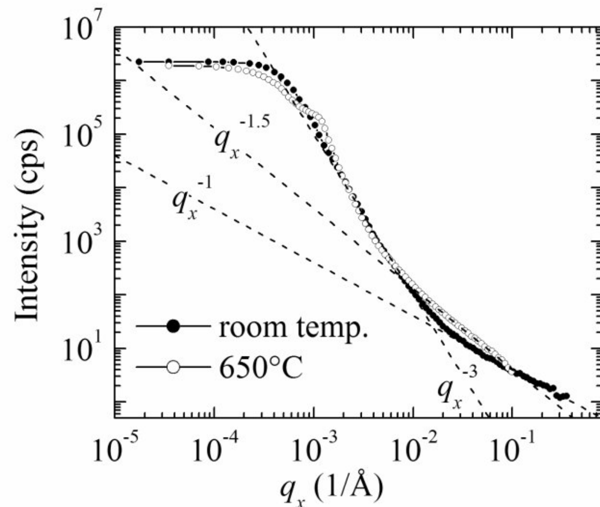

Figure 3. The q_x-scans in diffraction 333 measured at room temperature and at 650°C.

Acknowledgements

This work is a part of the research program MSM 0021622410 that is financed by the Ministry of Education of the Czech Republic; the assistance of O. Caha (Brno) in the X-ray experiments is appreciated. The Si wafers were kindly provided by ON SEMI Ltd., Rožnov p. Radh., Czech Republic.

References

1. M. A, Krivoglaz, *Diffuse Scattering of X-Rays and Neutrons by Real Crystals.* New York: Springer 1996.
2. L. A. Charnyi, K. D. Sherbachev, and V. T. Bublik, phys. stat. sol. (a), **128**, (1991), 303.
3. U. Pietsch, V. Holý, and T. Baumbach, *High-Resolution X-Ray Scattering: From Thin Films to Lateral Nanostructures.* NewYork: Springer 2004.
4. B. E. Warren, *X-ray Diffraction.* London: Dover Publ. 1990.
5. B. C. Larsson and W. Schmatz, Phys. Rev. B, **10**, (1974), 2307.
6. K. F. Kelton, R. Falster, D. Gambaro, M. Olmo, M. Cornara, and P. F. Wei, *J. Appl. Phys.*, **85**, (1999), 8097.